

1 **An efficient hierarchical model for multi-source information**
2 **fusion**

3 Ismaïl Saadi^{1*}, Bilal Farooq², Ahmed Mustafa¹, Jacques Teller¹, Mario Cools^{1,3,4}

4 ¹Local Environment & Management Analysis (LEMA), Urban and Environmental Engineering
5 (UEE), University of Liège, Allée de la Découverte, Quartier Polytech, 4000 Liège, Belgium

6 ²LITrans, Ryerson University, Department of Civil Engineering, 350 Victoria St, Toronto, Ontario
7 M5B 2K3, Canada

8 ³KULeuven Campus Brussels, Department of Informatics, Simulation and Modeling, Warmoesberg
9 26, 1000 Brussels, Belgium

10 ⁴Hasselt University, Faculty of Business Economics, Agoralaan Gebouw D, 3590 Diepenbeek,
11 Belgium

12 Email addresses: ismail.saadi@uliege.be (I. Saadi), bilal.farooq@ryerson.ca (B. Farooq),
13 a.mustafa@uliege.be (A. Mustafa), jacques.teller@uliege.be (J. Teller),
14 mario.cools@{uliege.be,kuleuven.be,uhasselt.be} (M. Cools)

15 *Corresponding author: Tel. : +32 4 366 96 44, Fax : +32 4 366 29 09

16 **Abstract**

17 In urban and transportation research, important information is often scattered over a wide variety
18 of independent datasets which vary in terms of described variables and sampling rates. As activity-
19 travel behavior of people depends particularly on socio-demographics and transport/urban-related
20 variables, there is an increasing need for advanced methods to merge information provided by multiple
21 urban/transport household surveys. In this paper, we propose a hierarchical algorithm based on a
22 Hidden Markov Model (HMM) and an Iterative Proportional Fitting (IPF) procedure to obtain
23 quasi-perfect marginal distributions and accurate multi-variate joint distributions. The model allows
24 for the combination of an unlimited number of datasets. The model is validated on the basis of a
25 synthetic dataset with 1,000,000 observations and 8 categorical variables. The results reveal that
26 the hierarchical model is particularly robust as the deviation between the simulated and observed
27 multivariate joint distributions is extremely small and constant, regardless of the sampling rates and
28 the composition of the datasets in terms of variables included in those datasets. Besides, the presented
29 methodological framework allows for an intelligent merging of multiple data sources. Furthermore,
30 heterogeneity is smoothly incorporated into micro-samples with small sampling rates subjected to
31 potential sampling bias. These aspects are handled simultaneously to build a generalized probabilistic
32 structure from which new observations can be inferred. A major impact in term of expert systems
33 is that the outputs of the hierarchical model (HM) model serve as a basis for a qualitative and
34 quantitative analyses of integrated datasets.

35 *Keywords.* Iterative Proportional Fitting (IPF); Hidden Markov Model (HMM); Hierarchical Model
36 (HM); Multi-source information fusion

37 1. Introduction

38 Forecasting activity-travel patterns is relevant to many applications and research domains, e.g.
39 urban/transportation research, and social sciences (Liu et al., 2013, 2015; Saadi et al., 2017). The
40 behavioral realism associated to the simulation of complex urban and transportation systems requires
41 highly disaggregated and reliable datasets (Batty, 2007; Axhausen & Gärling, 1992). A major problem
42 is that such disaggregated data are not always available (Barthelemy & Toint, 2013). Moreover,
43 sampling rates are generally low, i.e. in the best case at most 10% of the total population, as
44 data collection for travel surveys/micro-samples is costly, and large-scale surveys, i.e. censuses, are
45 systematically subjected to privacy and confidentiality issues (Saadi et al., 2016b). Therefore, in
46 urban and transportation research, efficient and flexible methods are required to fuse information
47 stemming from multiple micro-samples and aggregate statistics, e.g. socio-demographic marginal
48 distributions (Saadi et al., 2016b; El Faouzi et al., 2011; Saadi et al., 2016a; Wu, 2009).

49 In this paper, a methodological framework is presented that allows for an intelligent merging of
50 multiple data sources. Furthermore, heterogeneity is smoothly incorporated into micro-samples with
51 small sampling rates subjected to sampling bias. These aspects are handled simultaneously to build
52 a generalized probabilistic structure from which new observations can be inferred. A major impact in
53 term of expert systems is that the outputs of the hierarchical model (HM) model serve as a basis for
54 a qualitative and quantitative analysis of integrated datasets. In this context, the decision-making
55 process can be significantly simplified. Advanced knowledge for extracting relevant information from
56 multiple datasets could be replaced by a simpler analysis of a unified dataset that incorporates all
57 the information and variable interactions.

58 Section 1.1 presents a general overview of the existing methods. Section 1.2 lists the contributions
59 of the current study with respect to the existing work.

60 1.1. Related work

61 In the literature, four types of methods - synthetic reconstruction, combinatory optimization
62 (CO), sample free fitting, Monte Carlo Markov Chain (MCMC) simulation-based method - have been
63 distinguished (Ye et al., 2017) to merge data from multiple data sources.

64 IPF sythetic reconstruction-based approaches are commonly used for modeling populations for
65 transport and urban systems (Arentze et al., 2007; Beckman et al., 1996; Zhu & Ferreira, 2014;
66 Barthelemy & Toint, 2013). IPF procedures consist of fitting a multi-dimensional contingency table
67 given a set of target marginal distributions and a single micro-sample derived, for instance, from a
68 travel survey. Observed marginal distributions are used as targets for fitting the micro-sample via an
69 iterative reweighting procedure. In practice, the contingency tables are initiated with micro-samples
70 with low sampling rates, i.e. at most 5 to 10%. This dependency on micro-samples is particularly
71 problematic as IPF procedures systematically preserve the error of the related multi-variate joint
72 distribution despite the fact that the marginals are fitted quasi-perfectly. Furthermore, applying an
73 IPF may be problematic in the case of unavailable micro-samples for disaggregate inputs. In addition,
74 the quality of the sample influences the final IPF output. In some situations, when a combination
75 of attributes with low probability occurrence is missing within the sample, the synthetic population
76 will not include the corresponding set of combined attributes. Setting up the zero element cells with
77 very small values has been proposed to tackle this issue; however this would add an arbitrary bias. In
78 contrast, IPF procedures are particularly powerful in providing highly accurate synthetic populations,
79 when the correspondence between the synthetic and observed populations is evaluated on the basis
80 of the marginal distributions.

81 Besides, CO can be defined as a micro-data reconstruction approach which performs a random
82 selection of households from micro-samples in order to reproduce the characteristics of a specific

83 geographical unit. Different statistical metrics have been proposed to assess the goodness-of-fit of the
84 model (Voas & Williamson, 2000). Similar to IPF, CO is a sample-based approach that also suffers
85 from the zero-cell problem in the image of IPF.

86 Given the fact that disaggregated samples are difficult to obtain in some countries, sample-free
87 methods emerged as interesting alternatives. Marginal and/or conditional distributions of partial
88 attributes are adopted as input data in order to enable more flexibility. However, when the distribu-
89 tions are not consistent across the data sources, a problem occurring especially in the case of discrete
90 variables, further adjustments are operated by performing individual shifts. Furthermore, sample-free
91 methods are extremely time-consuming and generally require a heavy methodological procedure with
92 multiple connected sub-models for generating an individual pool.

93 With respect to the Markov Process-based methods, Farooq et al. (2013) used, for instance, an
94 MCMC method for population synthesis. Both the full and partial conditional distributions used by
95 MCMC method can be calibrated on multiple micro-samples. Despite the relative flexibility in terms
96 of data integration, the MCMC-based approach is insufficiently adapted for dealing with datasets
97 that have variables with a high number of categories. This is due to the fact that the Multinomial
98 Logit Models (MNL), that are used within the simulation procedure, are too sensitive to this type
99 of variables. In addition, the method may over-fit the micro-samples if full conditional probability
100 distributions are used and substantial information may be lost if partial conditionals are adopted.
101 Besides, MCMC simulation-based method can be considered as a sample-free approach as it relies on
102 conditional distributions which are calibrated on the basis of different data sources. Both discrete and
103 continuous variables can be handled. However, inconsistencies in conditional distributions, may keep
104 MCMC from converging towards a stationary state; which would never result in a correct population.

105 Saadi et al. (2016b) used an HMM-based approach for synthesizing the population of Belgium.
106 The method is highly flexible for fusing multiple micro-samples and shows competitive prediction
107 capabilities. Nonetheless, the full dependency on micro-samples often leads to less accurate simulated
108 marginal distributions despite accurate simulated joint distributions. In this paper, we propose an
109 extension of the HMM by integrating IPF, allowing an efficient multi-source information fusion.

110 *1.2. Contributions*

111 The contributions of the current study are defined as follows:

- 112 1. We develop a new hierarchical model for fusing an unlimited number of information sources
113 irrespective of the level of aggregation.
- 114 2. The hierarchical model generalizes the HMM by incorporating IPF. In doing so, the quality of
115 the simulated multivariate joint distributions is preserved in addition to quasi-perfect marginal
116 joint distributions.
- 117 3. Efficient algorithms are designed for smartly calibrating the hierarchical model (HM).

118 The remainder of the paper is structured as follows. First, we describe the new modeling frame-
119 work. In Section 3, the results are discussed and conclusions are formulated in Section 4.

120 **2. The Hierarchical Model (HM)**

121 *2.1. Data*

122 The methodology developed under the present study essentially handles (a) travel surveys which
123 include socio-demographics or transport/urban-related variables and (b) corresponding aggregate
124 marginal distributions. The variables can be either discrete or continuous but discretized to be

125 handled within the model. Typically, gender (male-female), car ownership (yes-no), socio-professional
126 status (student, worker, employee, etc.), residential location (ID of the commune) are, among others,
127 considered as discrete variables. The surveys may also include continuous variables such as age -
128 between 1 and 100 or travel time. In most cases, continuous variables are discretized into categories in
129 order to enable data fusion. In practice, researchers mainly deal with discrete or discretized continuous
130 variables. Data can be collected by means of face to face interviews or on-line questionnaires.

131 Besides, two types of input must be clearly distinguished in the current modeling framework.
132 On the one hand, we have the micro-samples, e.g. travel surveys, which are relatively detailed but
133 with small sampling rates, i.e. less than 10%. Also, the links in-between the variables are preserved
134 as for each observation, one has information about, e.g. gender, age, socio-professional status and
135 many other variables, of a specific anonymized person. On the other hand, we have aggregate data
136 which can be derived from national organisms or bureau of statistics independently of each other,
137 e.g. pyramid of ages, gender distribution, etc.

138 *2.2. Model structure*

139 The structure of the hierarchical model (HM), which enables multi-source information fusion, is
140 illustrated in Figure 1. HM includes two important components, i.e. HMM and IPF. The N micro-
141 samples and the M aggregate marginal distributions can be used simultaneously as inputs within the
142 HM framework. The scaled-up and fused micro-sample enables the connection between HMM and
143 IPF. As the multi-source fusion process already takes place within the HMM component, the scaled-
144 up and fused micro-sample systematically includes all the variables of interest. IPF enables a direct
145 fitting of the marginal distributions based on the observed targets, i.e. second set of inputs. Of course,
146 the use of all the aggregate marginal distributions is not mandatory. It depends on data availability.
147 Thus, HM is designed to allow enough flexibility towards unavailable marginal distributions. It is
148 indeed possible to fit data against a number of marginal distributions which is lower than the total
149 number of variables of interest, i.e. M . Finally, HM results in a fused and more accurate dataset that
150 can be used in multiple applications, e.g. agent-based modeling of complex urban and transportation
151 systems (Batty, 2007; Horni et al., 2016).

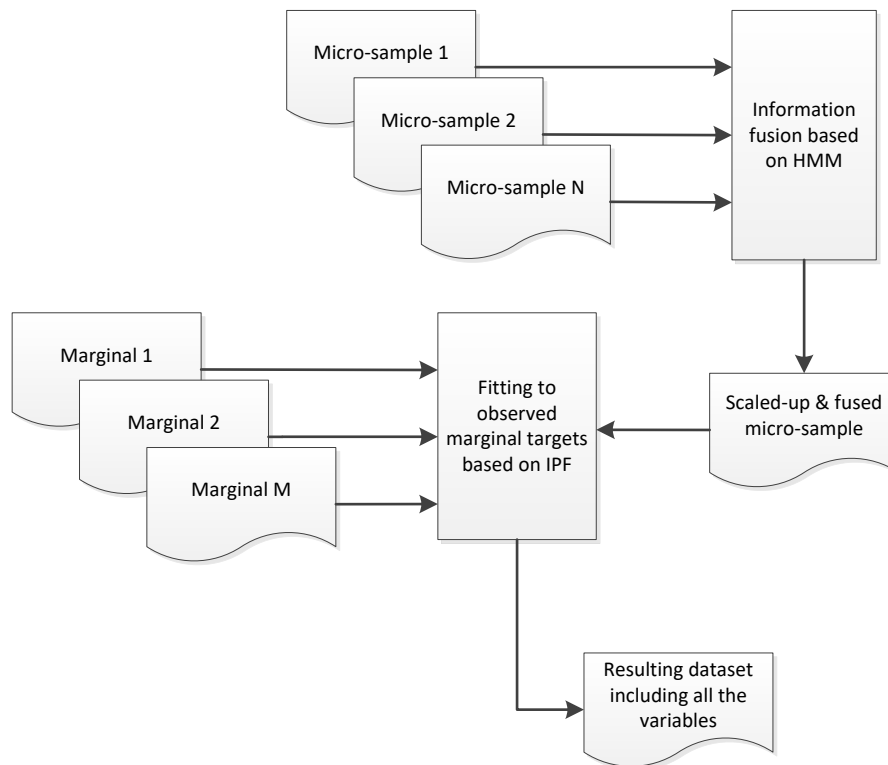


Figure 1: Structure of the hierarchical model

152 Regarding the fusion process, the N micro-samples are merged based on HMM using Algorithms
 153 1 and 2. In doing so, the HMM sequentially learns the configuration structure of the pseudo multi-
 154 variate joint distribution of the true population. Here, the word "pseudo" has been used because a
 155 sample with a very small sampling rate will never statistically replicate an accurate representation of
 156 the true population.

157

158 2.3. Learning

159 A new generalized algorithm is proposed in the context of this modeling framework to merge mul-
 160 tiple data sources and handle missing values, i.e. not attributed (NA) and/or not-a-number (NaN).
 161 Indeed, (a) standard methods for estimating HMM are not adapted for handling data stemming from
 162 multiple sources. Instead of estimating the transition probabilities from a single micro-sample, the
 163 algorithm is designed such that the information about the transition probabilities from a variable to
 164 another are extracted from their corresponding data source.

165 In addition, (b) the way of handling missing data vary from a method to another. A naive
 166 way is to clear the row with partial information. For example, a full observation, e.g. row in a
 167 dataset, containing a single NA value can be cleared. This may be problematic if missing values are
 168 important within the dataset. The overall distributions of the variables contained within the "cleaned
 169 sample" might be subjected to major changes compared to the original one. Thus, even if the dataset
 170 includes observations with partial information, then HMM ignores NA or NaN values and uses the

171 complementary available information for updating the model. This feature is enabled by Algorithm
172 2.

173 Two hypotheses have been formulated. (A1) In the case of a multi-source information fusion
174 operation, we assume that the different micro-samples share at least a common variable in order to
175 enable the shift from a sample to another, and for guarantying the fusion process. (A2) The categories
176 within the variables are defined as integers starting from 1.

177 In order to understand the fusion process, Figure 2 presents an HMM with n variables. The
178 variables are symbolized with states and the transition patterns with either continuous or dashed
179 arrows. For example, setting up a synthetic dataset of 3 variables, e.g. age, gender, car ownership,
180 would require an HMM of length 3, i.e. $n = 3$. The transition probabilities, $T_1, T_2, \dots, T_i, \dots, T_n$,
181 which can also be defined as 2 way tables are estimated from a single data source if all the variables are
182 included within the same dataset, from multiple datasets otherwise. For example, the link between
183 age and gender would come from sample 1 and the link between car ownership and gender or age
184 and car ownership from sample 2. In both cases, assumption A1 is respected as both samples share
185 at least a common variable. Detailed descriptive aspects have been included within the Algorithms
186 1, 2 and 3 to understand how the algorithms are applied.

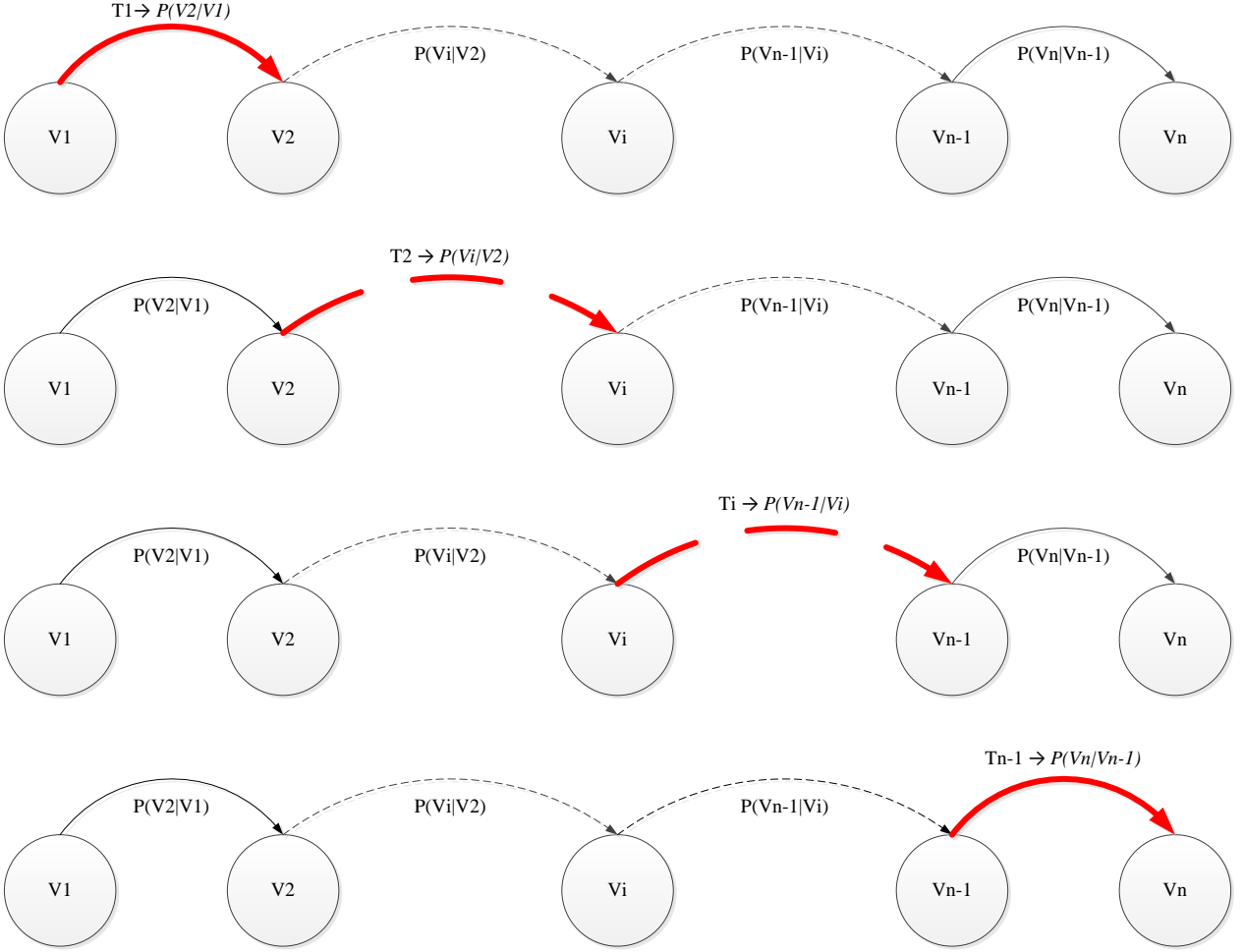


Figure 2: Representation of the transition patterns - V_i represents a variable with a specific number of categories. The objective is to systematically determine the relation between two adjacent variables by estimating a 2 way table. The red continuous-dashed arrows symbolize the transition patterns. They can either be estimated from a single or a combination of datasets. T_i represents a matrix which dimensions depend on the number of categories of the involved variables V_i and V_{i+1} .

187 Before running Algorithm 1, a pre-processing of the variables of interest should be realized. After
 188 selecting the variables, the micro-samples in which the variables are contained should be collected, e.g.
 189 from national travel surveys. The link between the transition patterns and their corresponding micro-
 190 samples needs to be clearly identified. Also, it must be ensured that common variables exist across
 191 the samples (Assumption 1) and that the categories are represented in terms of integers starting from
 192 1 (Assumption 2). Finally, the location of the partial transition matrix T_k needs to be pre-defined to
 193 enable the sequential updating of T .

Algorithm 1 Updating of the transition probability matrix T

```
// Initialize K number of transition patterns
// Initialize N sum over all the variable categories
Set K and N

// Returns an N×N matrix
T ← CreateTable(N,N)

// Loop over the K transition patterns
for k=1 to K-1 do
  // Returns a two-columns sample with variables  $V_k$  and  $V_{k+1}$ 
   $[V_k, V_{k+1}] \leftarrow \text{GetMicroSample}(k)$ 

  // Returns the corresponding two-way table  $P(V_{k+1}|V_k)$ 
   $T_k \leftarrow \text{Get2DCrossTab}(V_k, V_{k+1})$ 

  // Returns X-Y initial and final locations of  $T_k$  with respect to T
   $[xi, xf, yi, yf] \leftarrow \text{GetPositions}(k)$ 

  // Assign  $T_k$  to T within the corresponding location
   $T[xi \rightarrow xf, yi \rightarrow yf] \leftarrow T_k$ 
end for
```

Algorithm 2 Get2DCrossTab

```
function: Get2DCrossTab( $V_k, V_{k+1}$ )

// Returns the number of levels within the input variable
nk1 ← getNumberOfCategories( $V_k$ )
nk2 ← getNumberOfCategories( $V_{k+1}$ )

Tk ← CreateTable(nk1, nk2)

for i=1 to length( $V_k$ ) do
  if  $V_k[i] = \text{"NAN"}$  or  $V_{k+1}[i] = \text{"NAN"}$  or  $V_k[i] = \text{"NA"}$  or  $V_{k+1}[i] = \text{"NA"}$  then
    // Do not update
  else
     $Tk[V_k[i], V_{k+1}[i]] \leftarrow Tk[V_k[i], V_{k+1}[i]] + 1$ 
  end if
end for
return Tk
```

194 *2.4. Sampling*

195 After the learning step, a desired number of observations is inferred from the estimated HMM
196 structure using Algorithm 3. Theoretically, an infinite number of sequences can be generated based
197 on the estimated HMM while preserving all the properties of the population/original dataset. In

198 practice, it will depend on the application needs. In urban and transportation research, the number
 199 of sequences depends on the size of the populations that we need to synthesize. A sequence is defined
 200 as a combination of attributes or variables.

201 Algorithm 3 describes the adopted procedure for generating combination of attributes from the
 202 HMM component of HM. Based on the function `getDistribution()`, the distribution of V_1 is ob-
 203 tained and stored in \mathbf{p} . Q stands for the size of the population or the number of observations
 204 needed. After initializing the variables, we double loop along the columns and rows of A to generate
 205 sequentially the combination of attributes of the synthetic dataset.

Algorithm 3 Data sampling

Set Q // Number of observations - size of the dataset

// Returns the density distribution of variable V_1

$\mathbf{p} \leftarrow \text{GetDistribution}(V_1)$

// Returns null table of dimensions $Q \times K+1$ to store the set of observations

$A \leftarrow \text{CreatTable}(Q, M)$

for $j=1$ to Q do

$\gamma \leftarrow \text{Sample from } \mathbf{p}$

$A[j, 1] \leftarrow \gamma$

 for $k=1$ to K do

 // Returns the k th transition table T_k of T

$T_k \leftarrow \text{GetTransitionTable}(k, T)$

 Sample V_{k+1} from $T_k = P(V_{k+1}|V_k)$ based on V_k (or $A[j, k]$) and store in $A[j, k+1]$

 end for

end for

206 *2.5. Fitting*

207 After the sampling, the scaled-up and fused micro-sample is fitted to the target marginal distribu-
 208 tions to operate the final step of the HM modeling framework. In doing so, an adjusted population/-
 209 dataset is obtained. Although the cells are updated until the target aggregate marginal distributions
 210 are fitted, there is no risk of losing the configuration structure of the multi-dimensional table. In
 211 this regard, Barthelemy & Toint (2013) highlighted that IPF preserves the correlation structure of
 212 populations based on the odd ratios technique. The preservation of the weights within contingency
 213 tables is demonstrated in details in Mosteller (1968).

214 **3. Numerical experiments**

215 The hierarchical model is tested based on a synthetic dataset of 1,000,000 observations and 8
 216 random variables with 128, 16, 8, 8, 4, 4, 3 and 2 categories respectively. Data are deliberately het-
 217 erogeneous and designed in the image of real world situations. In urban and transportation research,
 218 variables contain multiple categories for representing socio-demographics/transport-related variables.
 219 The number of categories is even more important if spatial information is included. Therefore, we also
 220 chose a complex categorical variable with 128 levels. Table 1 presents a detailed statistical description
 221 of the synthetic dataset.

222 Surveys might be subjected to missing information, e.g. encoding errors during data collection
223 or presence of NA/NAN values. This issue is particularly important as the systematic removal of a
224 combination of variables because of a missing one may lead to overall changes in terms of variable
225 distributions. This aspect has been deeply discussed in Saadi et al. (2016b) by utilizing the survey
226 on workforce. Indeed, data synthesis of a higher number of variables would increase the probability
227 of finding a higher number of missing values. Saadi et al. (2016b) outlined that for the synthesis
228 of three variables, the gender distribution was 49.55% and 50.45% for male and female respectively
229 after data cleaning. Regarding the synthesis of 6 variables, the distribution shifted towards 53.97%
230 and 46.03% after data cleaning. Furthermore, the synthesis of 6 variables has led to a huge decrease
231 in the sample size compared to the original size, i.e. $\Delta = -68\%$. Thus, in the current study, a better
232 algorithm has been defined to synthesize any number of attributes based on the original datasets.
233 In this regard, performing data cleaning is no longer necessary. Valuable amount of information is
234 preserved then.

Table 1: Statistical description of the synthetic dataset

Variable ID	Number of levels	Statistical description
1	128	Truncated normal distribution
2	16	Normal distribution with the following proportions: 1:2% -2:3% -3:4% -4:6% 5:7% -6:8% -7:9% -8:10% 9:10% -10:9% -11:8% -12:7% 13:6% -14:4% -15:3% -16:2%
3	8	Poisson distribution with the following proportions: 1:5% -2:12% -3:18% -4:20% 5:18% -6:14% -7:9% -8:5%
4	8	Poisson distribution with the following proportions: 1:11% -2:19% -3:22% -4:20% 5:14% -6:8% -7:4% -8:2%
5	4	Poisson distribution with the following proportions: 1:15% -2:27% -3:31% -4:27%
6	4	Poisson distribution with the following proportions: 1:10% -2:22% -3:32% -4:36%
7	3	Poisson distribution with the following proportions: 1:8% -2:35% -3:57%
8	2	1:45% -2:55%

235 In order to underline the influence of the sampling rate on model outputs, five bootstrap samples
236 are derived from the original dataset in the following order 10%, 5%, 1%, 0.1% and 0.06%. There is
237 no point in considering sampling rates higher than 10%, since such data are typically not available. In
238 Section 3.1, we present the practical procedure for model estimation using a single micro-sample and
239 all the marginals. The results are compared on the basis of the joint and marginal distributions to
240 highlight the performances of HM. In Section 3.2, we illustrate how to fuse multi-source information
241 based on another case study considering multiple micro-samples and all the marginal distributions.

242 3.1. Model estimation

243 To run Algorithms 1 and 2, we identify the positions of the partial matrices T_k based on the
244 number of levels (see Table 1). The full transition probability matrix T is of dimension $n \times n$ where

245 $n = 128 + 16 + 8 + 8 + 4 + 4 + 3 + 2 = 173$. The eight variables of the micro-sample are arranged in
 246 descending order of the number of categories and stored as a matrix of dimension $(\delta * 1,000,000) \times 8$
 247 where δ is the sampling rate. We need to compute seven 2-way tables - transition patterns - as 8
 248 variables are synthesized. T matrix is updated through a sequential read of the transition patterns.
 249 The values of each variable of V_k and V_{k+1} are used as subscripts by T_k for localizing the corresponding
 250 cell. If NA or NAN values are detected, then the algorithm does not update T_k . Thus, incomplete
 251 datasets can be used without cleaning procedure as they are implicitly handled by the HM model.

252 After estimating T , we run Algorithm 3 to generate a certain number of combination of attributes.
 253 In this case study, the generated dataset includes 1,000,000 observations to enable a direct comparison
 254 with the original one, see Table 1. It must be kept in mind that a single micro-sample and all the
 255 aggregate marginals are available in this case study. V_1 is the first random variable which contains
 256 128 categories. A value between 1 and 128 is sampled based on the weights vector \mathbf{p} . Then, we
 257 loop over the transition patterns to systematically sample the next value based on the corresponding
 258 two-way table T_k . T includes all the two-way transition tables to sample the next variable from the
 259 current one, see Algorithm 3.

260 In this case study, T is defined by means of 7 two-way tables as 8 variables are handled, i.e.
 261 $T_{1 \rightarrow 128 | 129 \rightarrow 144}$, $T_{129 \rightarrow 144 | 145 \rightarrow 152}$, $T_{145 \rightarrow 152 | 153 \rightarrow 160}$, $T_{153 \rightarrow 160 | 161 \rightarrow 164}$, $T_{161 \rightarrow 164 | 164 \rightarrow 168}$, $T_{164 \rightarrow 168 | 169 \rightarrow 171}$ and
 262 $T_{169 \rightarrow 171 | 172 \rightarrow 173}$. Note that $T_{1 \rightarrow 128 | 129 \rightarrow 144}$ is not reported because of its dimensionality 128×16 . The
 263 dimensions of each single table are associated to the number of categories of two adjacent variables.
 264 For example, variables 7 and 8 contain 3 and 2 categories, respectively. Thus, T is updated from
 265 rows 169 to 171 and from columns 172 to 173 using $T_{169 \rightarrow 171 | 172 \rightarrow 173}$ of dimensions 3×2 . The same
 266 updating procedure is applied for the rest of the tables using Algorithms 1 and 2. Figure 3 shows
 267 how the interactions are occurring in-between multiple adjacent variables. As highlighted earlier in
 268 the paper, the transition patterns are defined as 2-way tables or bi-variate joint distributions. Each
 269 cell of a table represents the frequency of a combination of two categorical variables within the overall
 270 number of transitions. For instance, if we consider V_5 and V_6 , then the dimension of the corresponding
 271 2D table is 4-by-4 and it contains 16 cells.

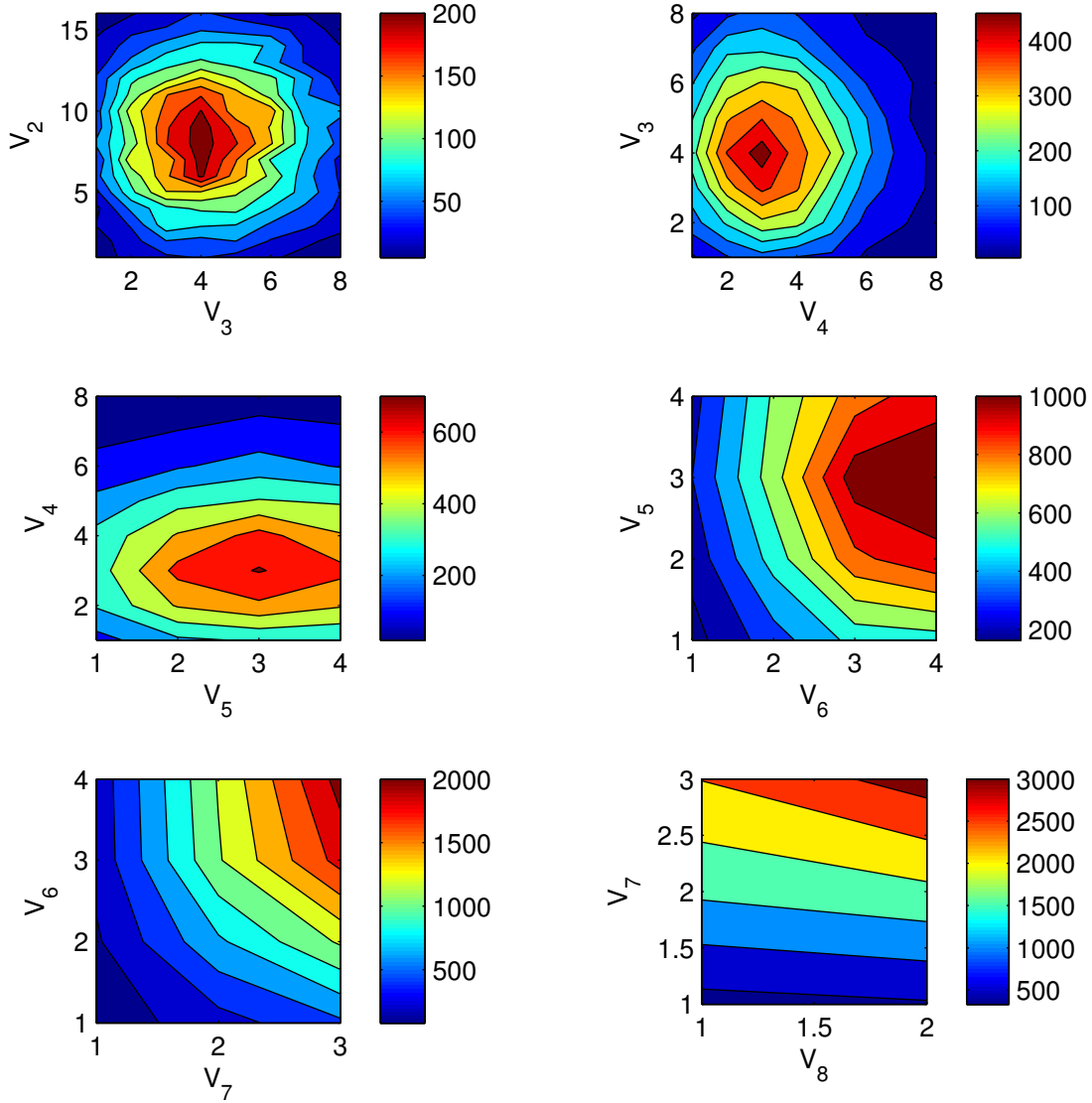


Figure 3: Variable interactions characterized by the probability matrix T , $T_{1 \rightarrow 128|129 \rightarrow 144}$, $T_{129 \rightarrow 144|145 \rightarrow 152}$, $T_{145 \rightarrow 152|153 \rightarrow 160}$, $T_{153 \rightarrow 160|161 \rightarrow 164}$, $T_{161 \rightarrow 164|164 \rightarrow 168}$, $T_{164 \rightarrow 168|169 \rightarrow 171}$ are respectively associated to the interaction maps $V_2 - V_3$, $V_3 - V_4$, $V_4 - V_5$, $V_5 - V_6$, $V_6 - V_7$, $V_7 - V_8$

272

273 The performance of the HM model that has been presented in this paper is compared with
 274 conventional methods reported in literature. In particular, the HM model is compared to the Direct
 275 Inflating (DI) approach, in which the sample is replicated multiple times to obtain the final dataset.
 276 In essence, the DI approach is a basic scaling-up process. A second comparison is made with Iterative
 277 Proportional Fitting (IPF,) as presented in Beckman et al. (1996). The comparison is made with
 278 Hidden Markov Models (HMM) (Saadi et al., 2016b).

279 Tables 2 and 6 present the marginal errors according to the benchmark methods (DI, IPF, HMM)
 280 and the new HM approach presented in this paper. One could depict that HM achieves comparable

281 results to that of IPF with quasi-perfect marginals. In contrast, DI and HMM show important
 282 deviations. Moreover, the evolution of the marginal errors demonstrates that there is a relationship
 283 between variable dimensionality and importance of the RMSE. Also the RMSE increases if sampling
 284 rate decreases.

Table 2: RMSE according to the marginals based on DI, IPF, HMM and HM for a sampling rate of 10%

	DI	IPF	HMM	HM
M1	274.36	1.67E-12	281.64	2.48E-11
M2	651.12	4.46E-12	614.60	9.70E-11
M3	937.42	1.03E-11	777.41	1.48E-11
M4	1080.50	1.03E-11	1061.53	0
M5	1419.66	0	1301.56	0
M6	762.06	0	826.85	7.28E-12
M7	651.80	0	283.25	8.42E-12
M8	1954.00	0	2165.00	4.12E-11

Table 3: RMSE according to the marginals based on DI, IPF, HMM and HM for a sampling rate of 5%

	DI	IPF	HMM	HM
M1	336.18	2.06E-11	360.05	3.19E-10
M2	785.28	2.50E-11	768.66	2.06E-10
M3	772.67	1.65E-11	799.21	2.53E-11
M4	830.02	1.56E-11	1009.45	1.80E-11
M5	2182.65	3.25E-11	2158.18	3.25E-11
M6	1177.64	3.00E-11	1115.92	0
M7	186.40	0	1037.01	0
M8	464.00	0	242.00	0

Table 4: RMSE according to the marginals based on DI, IPF, HMM and HM for a sampling rate of 1%

	DI	IPF	HMM	HM
M1	876.90	1.91E-11	882.35	6.31E-11
M2	3804.71	2.67E-11	3901.08	8.24E-12
M3	3193.39	1.31E-11	3111.55	1.50E-11
M4	2941.89	1.82E-11	2901.29	1.07E-11
M5	2757.62	3.25E-11	3065.11	0
M6	4400.60	2.91E-11	4254.56	3.25E-11
M7	7349.19	3.36E-11	7234.25	3.46E-11
M8	8164.00	8.23E-11	7856.00	0

Table 5: RMSE according to the marginals based on DI, IPF, HMM and HM for a sampling rate of 0.1%

	DI	IPF	HMM	HM
M1	3546.39	1.70E-11	3555.91	2.14E-09
M2	13461.83	1.59E-11	13448.65	1.10E-11
M3	7254.36	2.37E-11	7242.95	1.80E-11
M4	11203.24	1.90E-11	11122.91	1.06E-11
M5	12686.65	4.37E-11	12700.80	1.46E-11
M6	12677.68	2.91E-11	12542.79	0
M7	18078.30	3.36E-11	18499.72	8.40E-12
M8	29264.00	4.12E-11	30059.00	0

Table 6: RMSE according to the marginals based on DI, IPF, HMM and HM for a sampling rate of 0.06%

	DI	IPF	HMM	HM
M1	3546.39	1.70E-11	3555.91	2.14E-09
M2	13461.83	1.59E-11	13448.65	1.10E-11
M3	7254.36	2.37E-11	7242.95	1.80E-11
M4	11203.24	1.89E-11	11122.91	1.06E-11
M5	12686.65	4.37E-11	12700.80	1.46E-11
M6	12677.68	2.91E-11	12542.79	0
M7	18078.30	3.36E-11	18499.72	8.40E-12
M8	29264.00	4.11E-11	30059.00	0

285 In order to investigate the propagation of the error through the HM, Table 7 presents the RMSE
 286 for different sampling rates based on DI, IPF, HMM and HM. DI means that the bootstrap sample
 287 has been directly scaled-up and compared to the observed dataset. RMSE of DI and IPF are almost
 288 equivalent because IPF re-weights the contingency tables with respect to targets while preserving
 289 the proportions. Thus, even the related errors are preserved. Also, HM and HMM show equivalent
 290 RMSE's for the three highest sampling rates. In the case of the extremely small sampling rate,
 291 i.e. 0.06%, a slight deviation can be observed because of the reweighting procedure enabled by IPF.
 292 Theoretically the errors of HMM and HM should be exactly the same as highlighted in Section 2, but
 293 small differences are observed. This can be explained by the fact that at the end of the reweighting of
 294 the multi-dimensional contingency table, the cell values are rounded. As the later contingency table
 295 contains a huge number of cells, the cumulation of rounding error leads to a small decrease of the
 296 errors especially for small sampling rates.

Table 7: Evolution of the RMSE according to multiple sampling rates and methods

	DI	IPF	HMM	HM
10%	0.85	0.85	0.40	0.40
5%	1.23	1.23	0.40	0.40
1%	2.81	2.83	0.40	0.41
0.1%	8.91	10.00	0.45	0.49
0.06%	11.5	13.65	0.49	0.54

297 Based on the results of Tables 2-6 and 7, we conclude that HM allows the best trade-off as multi-
 298 variate joint distribution errors are almost preserved as well as those of the marginals. Also, HM is

299 less sensitive to sampling rate variability, i.e. from 10% to 0.06%, as the RMSE increases by +35%.
 300 When IPF is considered independently, the RMSE increases by +1505.88%. The results reveal that
 301 the IPF component of HM affects only the marginals but HMM influences the multi-variate joint
 302 distribution. This can be explained by the fact that the HMM component of HM incorporates more
 303 heterogeneity into the micro-sample. Indeed, for small sampling rates, some combination of attributes
 304 are not necessarily covered. This problem is implicitly avoided by HM.

305 3.2. Multi-source information fusion

306 In this second case study, we suppose that the dataset that we want to synthesize contains the
 307 same number of variables and variable categories. The only difference is that the variables are included
 308 within 3 independent datasets in order to illustrate how to perform a multi-source information fusion.
 309 Table 8 presents the distribution of the variables through the 3 micro-samples (MS) with different
 310 sampling rates. The sampling rates are deliberately low in order to highlight how efficient is the HM.
 311 Each single micro-sample contains four variables.

Table 8: Description of the micro-samples (*MS*)

	<i>MS1</i>	<i>MS2</i>	<i>MS3</i>
<i>M1</i>			×
<i>M2</i>	×		×
<i>M3</i>	×		
<i>M4</i>	×		×
<i>M5</i>		×	×
<i>M6</i>		×	
<i>M7</i>		×	
<i>M8</i>	×	×	
Sampling rate	0.1%	1.0%	2.0%

312 Based on Table 8, we notice that $T_{1 \rightarrow 128|129 \rightarrow 144}$, $T_{129 \rightarrow 144|145 \rightarrow 152}$, $T_{145 \rightarrow 152|153 \rightarrow 160}$, $T_{153 \rightarrow 160|161 \rightarrow 164}$,
 313 $T_{161 \rightarrow 164|164 \rightarrow 168}$, $T_{164 \rightarrow 168|169 \rightarrow 171}$ and $T_{169 \rightarrow 171|172 \rightarrow 173}$, can be estimated with *MS3* (micro-sample 3),
 314 *MS1*, *MS1*, *MS3*, *MS2*, *MS2*, *MS2* respectively using Algorithms 1 and 2. In doing so, T is fully
 315 implemented based on partial micro-samples. Also, multi-source information fusion is made effective.
 316 The rest of the procedure is similar to what has been described in Section 3.2. Figure 4 presents the
 317 comparison between the simulated and observed datasets on the basis of the marginals. One could
 318 depict that HM leads to quasi-perfect marginals regardless of the variable complexity.

319 In addition, Figure 5 shows the comparison between the simulated and observed multi-variate joint
 320 distributions for different combination of variable patterns. There is no risk of under/over-estimation
 321 as the data points present a good symmetry on both sides of the straight line. Moreover, linear fits (in
 322 red) and straight lines (in green) are almost systematically overlapped. Slopes are ranging from 0.97
 323 to 1.00 with extremely small intercepts. Important spread can be observed with respect to patterns
 324 $V_1 - V_2 - V_3$, $V_2 - V_3 - V_4$ and $V_3 - V_4 - V_5$ because of variable dimensionality. V_i are arranged in
 325 descending order of number of categories. Thus the combination $V_1 - V_2 - V_3$ has the highest number
 326 of cells. As a result, the density of data points is significant (Figure 5a).

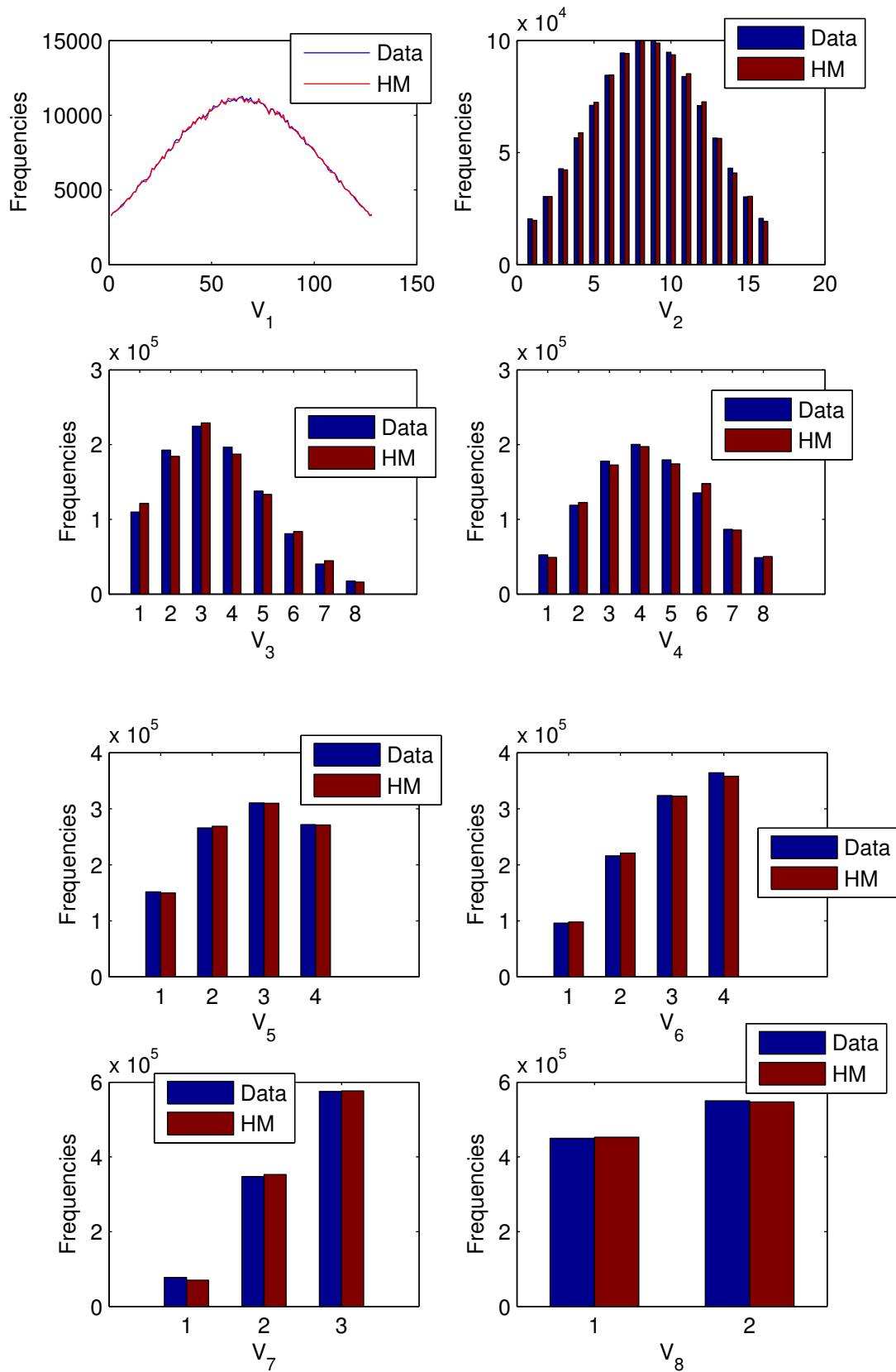
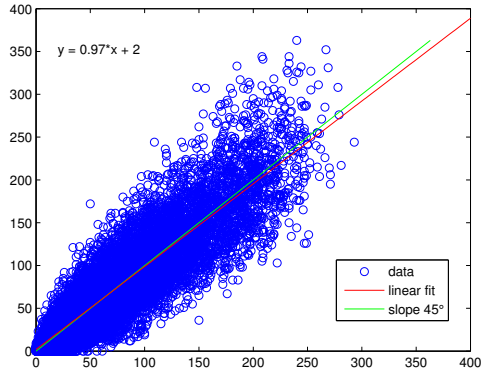
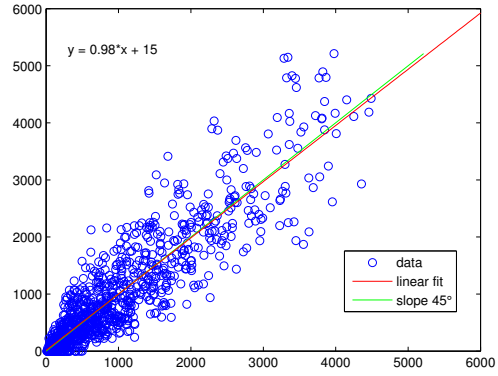


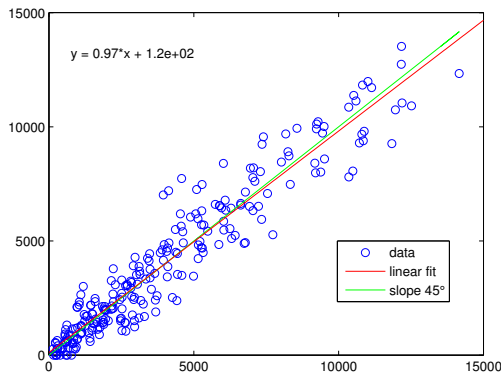
Figure 4: Comparison between the simulated and observed marginals



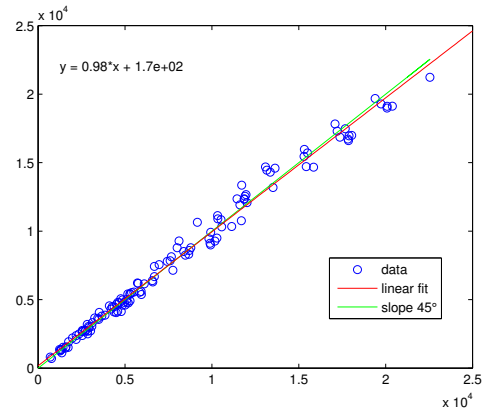
(a) $V_1 - V_2 - V_3$



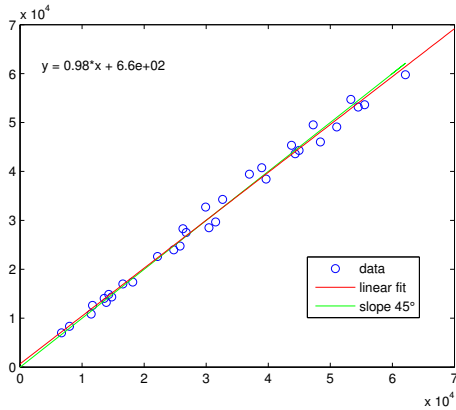
(b) $V_2 - V_3 - V_4$



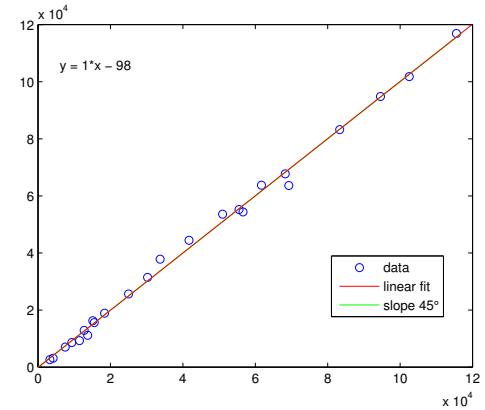
(c) $V_3 - V_4 - V_5$



(d) $V_4 - V_5 - V_6$



(e) $V_5 - V_6 - V_7$



(f) $V_6 - V_7 - V_8$

Figure 5: Comparison between the simulated and observed multi-variate joint distributions

3.3. Implications of the experimental outcomes

The experimental outcomes presented in the current study may have important implications in terms of modeling options. It has been now clearly demonstrated that (a) one should rather use a hierarchical procedure to ensure that the dataset is sufficiently accurate regardless the statistical indicators used. (b) Micro-samples may suffer from a lack of representativeness as combination of attributes with low probability of occurrence may not be captured during data collection. Thus,

333 the HMM component of the HM simultaneously merges multiple datasets in addition to incorpo-
 334 rating enough heterogeneity to avoid problems related to representativeness or sampling bias. (c)
 335 The presented framework would make the fusion process more straightforward for researchers and
 336 practitioners. (d) A major impact in term of expert systems is that the outputs of the HM model
 337 serve as a basis for a qualitative and quantitative analyses of integrated datasets. In this context, the
 338 decision-making process can be significantly simplified. Advanced knowledge for extracting important
 339 information from multiple datasets could be shifted towards a simpler analysis of a unified dataset
 340 that incorporates all the information and variable interactions.

341 *3.4. Theoretical comparison*

342 Table 9 compares HM with HMM and IPF in terms of the strengths and weaknesses based on
 343 several criteria. Aggregate data, e.g. populations age and gender distributions, are reliable and ex-
 344 tremely stable. Disaggregate data, e.g. household travel surveys, provide detailed information about
 345 people, but are generally subjected to small sampling rates leading to a serious lack of represen-
 346 tativity. HM clearly provides the best trade-off compared to the conventional IPF and the recent
 347 HMM-based approach.

	IPF	HMM	HM
Use of aggregate data	Yes	Partial	Yes
Use of disaggregate data	Partial	Yes	Yes
Quasi-perfect marginal distributions	Yes	No	Yes
Accurate multivariate joint distribution	No	Yes	Yes
Information fusion	Partial	Partial	Full

Table 9: Comparison between IPF, HMM and HM

348 **4. Conclusions**

349 In urban and transportation research, key information about agents, i.e. households or individuals,
 350 is often included within a wide range of small and independent datasets. To combine the information
 351 from these independent datasets, we presented a hierarchical model (HM) for (i) allowing multi-source
 352 information fusion and (ii) achieving higher prediction accuracies.

353 Based on the results highlighted in Section 3, the strengths of the proposed research can be
 354 formulated as follows:

- 355 • HM provides the best trade-off in terms of RMSE minimization, when marginals and joint
 356 distributions are simultaneously compared. This can be explained by the fact that the principal
 357 key features of IPF and HMM are combined within a single unified framework.
- 358 • Multiple micro-samples and aggregate marginals can be integrated within HM for allowing
 359 multi-source information fusion. Also HM shows a lot of flexibility in terms of data availability.
 360 We mentioned that a partial set of marginals can be used if there is absolutely no data.
- 361 • HM is extremely competitive and relatively robust with respect to sampling rate variability.
 362 This means that with a sampling rate of only 1%, it is possible to achieve results which are
 363 almost comparable to a HM calibrated with a micro-sample of 10%. Several applications within
 364 the field of urban and transportation research assume sampling rates which are around 1% using
 365 standard methods, i.e. IPF. But the results presented in Table 7 show that with IPF, a still

366 commonly used method, the RMSE is equal to 13.65. In this context, HM emerges as a far
367 better alternative for mitigating the error in micro-simulation.

368 Besides, further research is needed to overcome weaknesses of the proposed research method:

- 369 • Generalizing the method for handling a wide range of input data format is an important issue.
370 A systematic expert system procedure could be more efficient to enable intelligent data fusion
371 strategies. Indeed, although the developed fusion method provides interesting results, further
372 methodological improvements can be integrated within the modeling framework to make it
373 more universal. At this point, surveys and aggregate-based data are handled by the HM.
374 However, fusing the current data format with other types of data, e.g. panel data, GPS traces
375 of individuals, trip data is still a key challenge.
- 376 • The integration of a feature that allows for multi-level data fusion should be investigated.
377 For example, in transportation research, decision-making process can be explained at both
378 household and individual levels. Household data is more aggregated than individual level data.
- 379 • To extend the use of the current method within other research fields, additional efforts are
380 needed to ensure that HM is relatively robust to scalability, referred to as the number of
381 variables that should be synthesized. In this regard, an important issue raises up regarding the
382 interaction between scalability and the increase of heterogeneity. Is there a risk of getting a
383 reverse effect?

384 5. Acknowledgements

385 The research was funded by the ARC grant for Concerted Research Actions for project no. 13/17-
386 01 entitled "Land-use change and future flood risk: influence of micro-scale spatial patterns (Flood-
387 Land)" and by the Special Fund for Research for project no. 5128 entitled "Assessment of sampling
388 variability and aggregation error in transport models", both financed by the French Community of
389 Belgium (Wallonia-Brussels Federation).

390 6. References

- 391 Arentze, T., Timmermans, H., & Hofman, F. (2007). Creating synthetic household populations:
392 problems and approach. *Transportation Research Record: Journal of the Transportation Research*
393 *Board, 2014*, 85–91. doi:<https://doi.org/10.3141/2014-11>.
- 394 Axhausen, K. W., & Gärling, T. (1992). Activity-based approaches to travel analysis: conceptual
395 frameworks, models, and research problems. *Transport reviews, 12*, 323–341. doi:<http://dx.doi.org/10.1080/01441649208716826>.
- 397 Barthelémy, J., & Toint, P. L. (2013). Synthetic population generation without a sample. *Trans-*
398 *portation Science, 47*, 266–279. doi:<https://doi.org/10.1287/trsc.1120.0408>.
- 399 Batty, M. (2007). *Cities and complexity: understanding cities with cellular automata, agent-based*
400 *models, and fractals*. The MIT press.
- 401 Beckman, R. J., Baggerly, K. A., & McKay, M. D. (1996). Creating synthetic baseline populations.
402 *Transportation Research Part A: Policy and Practice, 30*, 415–429. doi:[https://doi.org/10.](https://doi.org/10.1016/0965-8564(96)00004-3)
403 [1016/0965-8564\(96\)00004-3](https://doi.org/10.1016/0965-8564(96)00004-3).

- 404 El Faouzi, N.-E., Leung, H., & Kurian, A. (2011). Data fusion in intelligent transportation systems:
405 Progress and challenges—a survey. *Information Fusion*, *12*, 4–10. doi:[https://doi.org/10.1016/
406 j.inffus.2010.06.001](https://doi.org/10.1016/j.inffus.2010.06.001).
- 407 Farooq, B., Bierlaire, M., Hurtubia, R., & Flötteröd, G. (2013). Simulation based population synthe-
408 sis. *Transportation Research Part B: Methodological*, *58*, 243–263. doi:[http://dx.doi.org/10.
409 1016/j.trb.2013.09.012](http://dx.doi.org/10.1016/j.trb.2013.09.012).
- 410 Horni, A., Nagel, K., & Axhausen, K. W. (2016). *The multi-agent transport simulation MATSim*.
411 doi:<https://doi.org/10.5334/baw>.
- 412 Liu, F., Janssens, D., Cui, J., Wets, G., & Cools, M. (2015). Characterizing activity sequences
413 using profile hidden markov models. *Expert Systems with Applications*, *42*, 5705–5722. doi:<https://doi.org/10.1016/j.eswa.2015.02.057>.
- 415 Liu, F., Janssens, D., Wets, G., & Cools, M. (2013). Annotating mobile phone location data with
416 activity purposes using machine learning algorithms. *Expert Systems with Applications*, *40*, 3299–
417 3311. doi:<https://doi.org/10.1016/j.eswa.2012.12.100>.
- 418 Mosteller, F. (1968). Association and estimation in contingency tables. *Journal of the American*
419 *Statistical Association*, *63*, 1–28. doi:<https://doi.org/10.1080/01621459.1968.11009219>.
- 420 Saadi, I., Mustafa, A., Teller, J., & Cools, M. (2016a). Forecasting travel behavior using markov
421 chains-based approaches. *Transportation Research Part C: Emerging Technologies*, *69*, 402–417.
422 doi:<https://doi.org/10.1016/j.trc.2016.06.020>.
- 423 Saadi, I., Mustafa, A., Teller, J., & Cools, M. (2017). Investigating the impact of river floods on
424 travel demand based on an agent-based modeling approach: The case of liège, belgium. *Transport*
425 *Policy*, . doi:<https://doi.org/10.1016/j.tranpol.2017.09.009>.
- 426 Saadi, I., Mustafa, A., Teller, J., Farooq, B., & Cools, M. (2016b). Hidden markov model-based
427 population synthesis. *Transportation Research Part B: Methodological*, *90*, 1–21. doi:[https://
428 doi.org/10.1016/j.trb.2016.04.007](https://doi.org/10.1016/j.trb.2016.04.007).
- 429 Voas, D., & Williamson, P. (2000). An evaluation of the combinatorial optimisation approach to the
430 creation of synthetic microdata. *Population, Space and Place*, *6*, 349–366. doi:[https://doi.org/
431 10.1002/1099-1220\(200009/10\)6:5<349::AID-IJPG196>3.0.CO;2-5](https://doi.org/10.1002/1099-1220(200009/10)6:5<349::AID-IJPG196>3.0.CO;2-5).
- 432 Wu, S. (2009). Applying statistical principles to data fusion in information retrieval. *Expert Systems*
433 *with Applications*, *36*, 2997–3006. doi:<https://doi.org/10.1016/j.eswa.2008.01.019>.
- 434 Ye, P., Hu, X., Yuan, Y., Wang, F.-Y. et al. (2017). Population synthesis based on joint distribution
435 inference without disaggregate samples. *Journal of Artificial Societies and Social Simulation*, *20*,
436 1–16.
- 437 Zhu, Y., & Ferreira, J. (2014). Synthetic population generation at disaggregated spatial scales for
438 land use and transportation microsimulation. *Transportation Research Record: Journal of the*
439 *Transportation Research Board*, *2429*, 168–177. doi:<https://doi.org/10.3141/2429-18>.